Carbohydrate Polymers 101 (2014) 179–187

Contents lists available at ScienceDirect

Carbohydrate Polymers

journal homepage: www.elsevier.com/locate/carbpol

Hollow latex particles functionalized with chitosan for the removal of formaldehyde from indoor air

Sukanya Nuasaen[a], Pakorn Opaprakasit[b], Pramuan Tangboriboonrat[a,*]

[a] Department of Chemistry, Faculty of Science, Mahidol University, Rama 6 Road, Phyathai, Bangkok 10400, Thailand
[b] School of Bio-Chemical Engineering and Technology, Sirindhorn International Institute of Technology (SIIT), Thammasat University, Pathum Thani 12120, Thailand

ARTICLE INFO

Article history:
Received 20 July 2013
Received in revised form
15 September 2013
Accepted 18 September 2013
Available online 25 September 2013

Keywords:
Hollow latex particle
Formaldehyde adsorption
Chitosan
Polyethyleneimine

ABSTRACT

Chitosan and polyethyleneimine (PEI) functionalized hollow latex (HL) particles were conveniently fabricated by coating poly(methyl methacrylate-co-divinyl benzene-co-acrylic acid) (P(MMA/DVB/AA)) HL particles with 5 wt% chitosan or 14 wt% PEI. The materials were used as formaldehyde adsorbent, where their adsorbent activity was examined by Fourier Transform Infrared (FTIR) spectroscopy. The nucleophilic addition of amines to carbonyls generated a carbinolamine intermediate with a characteristic band at 1020 cm^{-1} and Schiff base product at 1650 cm^{-1}, whose intensity increased with prolonged formaldehyde exposure times. The major products observed in HL-chitosan were carbinolamine and Schiff base, whereas a small amount of Schiff base was obtained in HL-PEI particles, confirming a chemical bond formation without re-emission of formaldehyde. Compared to HL-PEI, HL-chitosan possesses higher formaldehyde adsorption efficiency. Besides providing opacity and whiteness, the multilayer HL-chitosan particles can effectively remove indoor air pollutants, i.e., formaldehyde gas, and, hence, would be useful in special coating applications.

1. Introduction

Formaldehyde, a colorless, flammable, and bad smelling gas, is a common precursor in production of more complex materials, e.g., phenol-formaldehyde and urea-formaldehyde resins, which are widely used as wood-binding products and insulating foam (Cogliano et al., 2005). Formaldehyde is also applied in plastics, coatings and textile finishing in spite of the fact that it is carcinogenic in humans (Cogliano et al., 2005; Formaldehyde TEACH Chemical Summary, http://www.epa.gov/teach/chem_summ/Formaldehyde_summary.pdf, 2013). When absorbed in the upper respiratory tract, it can be oxidized to formate and carbon dioxide or incorporated into biological macromolecules (Heack et al., 1985). At >6 ppm of formaldehyde, cellular proliferation increases and then amplifies the genotoxic effect (Cogliano et al., 2005). In addition, there is strong but not sufficient evidence that formaldehyde causes leukemia. Therefore, emitted formaldehyde gas in indoor air is considered hazardous and should be removed.

Among several methods used in the removal of formaldehyde in an indoor environment, e.g., decomposition using photocatalyst and physical adsorption by porous materials, one of the effective methods is chemical adsorption, where a re-emission is excluded due to strong chemical bonding (Agudo, Polo, Bernal, Coronas, & Santamaria, 2004; Obee & Brown, 1995; Wada, Uragami, & Matoba, 2005). Formaldehyde gas can be chemically adsorbed by polymeric amines, e.g., chitosan and polyethyleneimine (PEI) via a reaction of primary (1°) amines to form azomethine or Schiff base, a compound containing an aryl or alkyl carbon-nitrogen double bond (Da Silva et al., 2011; Gesser & Fu, 1990; Wada et al., 2005; Yang, Liu, Yu, & Chen, 2011). Enhancement of formaldehyde adsorption was achieved by increasing the content of amines in the adsorbent. Nonporous TiO_2 fiber functionalized with high PEI content showed high adsorbent efficiency, and was used as quartz crystal microbalance (QCM) sensors (Wang et al., 2012). Chitosan-hybridized acrylic resin was used as a binder in interior finishing coating for formaldehyde adsorption by employing the reaction between amino group of chitosan and carbonyl of formaldehyde (Wada et al., 2005). Most importantly, when the Schiff base is formed, adsorbed formaldehyde was not released from chitosan-hybridized acrylic resin film, even with heat treating the film at 60 °C for 2 h.

For preparation of chitosan-coated particles, colloidal particles having high surface area were used as a substrate to increase the amount of attached chitosan. As a cationic polymer, chitosan is conveniently coated onto oppositely charge colloidal particles, e.g., poly(styrene-co-acrylic acid) (P(St/AA)), via the Layer by Layer (LbL) technique. The thickness of the adsorbed chitosan layer

* Corresponding author. Tel.: +66 2 2015135; fax: +66 2 3547151.
E-mail addresses: sukanyanuasaen@hotmail.com (S. Nuasaen), pakorn@siit.tu.ac.th (P. Opaprakasit), pramuan.tan@mahidol.ac.th (P. Tangboriboonrat).

0144-8617/$ – see front matter © 2013 Elsevier Ltd. All rights reserved.
http://dx.doi.org/10.1016/j.carbpol.2013.09.059

increased when P(St/AA) particles containing a higher amount of carboxylic acid groups on the surface were employed (Du, Liu, Mu, & Wang, 2010). Chemical structure also has a strong effect on the coating efficiency. Compared to the high charge density linear poly(allylamine hydrochloride) (PAH), the lower charge density branched PEI formed a thicker layer on silica nanoparticles (Nypelo, Osterberg, Zu, & Laine, 2011).

In this study, carboxylated hollow latex (HL) polymer particles or void containing particles have hiding power due to multiple scattering between its surrounding medium and void, were used as a substrate for chitosan or PEI coating (Silva & Galembeck, 2010). The composite material was designed to combine both optical property and formaldehyde adsorption ability. Besides higher surface to volume ratio, the advantages of HL particles over conventional white pigments or opacifying agents are; lower density, better UV resistance, lower coefficient to thermal expansion, less agglomeration, and lower cost per gallon (Bourgeat-Lami, 2003; McDonald & Devon, 2002). Therefore, HL particles possessing high surface charge density and strong double shell are prepared via the template based strategy seeded emulsion polymerization, using P(St/AA) as a seed particle and methyl methacrylate (MMA)/divinyl benzene (DVB)/AA as monomers (Nuasaen & Tangboriboonrat, 2013). The spherical and non-collapsed HL particles having voids of ca. 280 nm in size are then coated with chitosan or PEI to produce HL-chitosan or HL-PEI particles via the LbL technique. The materials are used as formaldehyde adsorbent. The chemical composition, size, charge and morphology of HL-chitosan and HL-PEI particles are characterized by Fourier Transform Infrared (FTIR) spectroscopy, thermogravimetric analysis, dynamic light scattering, and transmission electron microscopy. Effect of type of polymeric amines on formaldehyde adsorption behaviors and the adsorption mechanism are also analyzed by FTIR spectroscopy.

2. Experimental

2.1. Materials

Styrene (St) (Sigma–Aldrich, Purum) and methyl methacrylate (MMA) (Fluka, Purum) were purified by passing through a column packed with neutral and basic aluminum oxide (Fluka, Purum), while acrylic acid (AA) (Aldrich, Purum) was distilled before use. Divinyl benzene (DVB) (Merck, Synthesis), potassium persulfate (KPS) (Fluka, Puriss), and 40% formaldehyde (Carlo Erba, Analysis) were used as received. Polyethyleneimine (PEI), MW of 750,000 g/mol (Aldrich, 50 wt% aqueous solution) was diluted to 2 wt%. Chitosan, MW of 22,000 g/mol (90% deacetylation) (Ta Ming Enterprise Co., Ltd., Thailand) was dissolved in 0.1 M acetic acid (Merck, Analysis). Deionized (DI) water was used throughout the work.

2.2. Preparation of seed and HL particles

P(St/AA) latex particles were synthesized by soap-free emulsion polymerization (Polpanich, Tangboriboonrat, & Elaissari, 2005). DI water (90 g) was bubbled with nitrogen for 30 min before adding St (10 g) and AA (1.5 g). The polymerization was started with the addition of KPS solution (0.1 g in 10 g of water) at 70 °C. After the reaction completion, the residual monomers, electrolyte and water-soluble oligomers were removed by centrifugation (12,000 rpm, 20 min) and washed thrice with DI water.

Highly-charged HL particles were prepared via seeded emulsion polymerization, as previously described (Nuasaen & Tangboriboonrat, 2013). P(St/AA) seed latex (0.523 g) was diluted to 36 g in total. After nitrogen purging for 30 min and heating to 80 °C, DVB (0.9 g) was added, followed by two portions of MMA/AA/KPS (0.95/0.1/0.007 g). The polymerization was carried out for 5 h. The resulting HL was washed thrice with DI.

2.3. Preparation and characterization of HL-chitosan and HL-PEI particles

The carboxylated HL particles were coated with chitosan and PEI by simply adding 1% (w/v) chitosan solution at pH 5 or 2% (w/v) PEI solution (2.0 ml) at pH 7 into 0.5% (w/v) HL (10.0 ml) while shaking (IKA, VIBRAX VXR basic) at room temperature for 12 h. The free chitosan or PEI was removed from HL-chitosan or HL-PEI by centrifugation (5000 rpm, 15 min) and washed twice with DI water. Their chemical composition, average size, zeta potential, and morphology were, respectively, characterized by using an FTIR spectrometer in the attenuated total reflection mode (ATR-FTIR; Thermo Scientific, iD5), thermogravimetric analysis (TGA; Mettler Toledo, SDTA851), dynamic light scattering (DLS; Zetasizer Malvern, Nano ZS) and transmission electron microscope (TEM; FEI, TECHNAI), operated at an accelerator voltage of 120 kV.

2.4. Formaldehyde adsorption test

The adsorption test was performed in a 500 ml chamber saturated with formaldehyde vapor, generated by heating a 40% formaldehyde solution at 80 °C, in the presence of chitosan, PEI, HL-chitosan, or HL-PEI samples previously dried at 60 °C for 24 h (Gesser & Fu, 1990). In order to ensure the saturation, formaldehyde vapor was filled into the empty chamber at 25 °C for 30 min before starting the first test and for 15 min before starting each consecutive test. After formaldehyde adsorption for 0–120 min, the samples were characterized by FTIR (FTIR; Perkin Elmer, Spectra GX) and ATR-FTIR (ATR-FTIR; Thermo Scientific, iD5). FTIR spectra of chitosan, HL-chitosan, and HL-PEI samples were collected on a single-reflection diamond/ZnSe ATR accessory, whereas those of PEI were examined in transmission mode by casting each sample on a Ge window.

3. Results and discussion

3.1. Analysis of amine functionalized HL particles

FTIR spectra of PEI, chitosan, HL, HL-PEI, and HL-chitosan are shown in Fig. 1.

The characteristic peaks at 3440 and 1558 cm^{-1} in Spectrum 1A correspond to N—H stretching and N—H vibration of PEI (Jenjob, Tharawut, & Sunintaboon, 2012). Spectrum 1B illustrates the characteristic bands at 3440 cm^{-1}, relating to O—H and N—H stretching, whereas two bands at 1650 and 1558 cm^{-1} are attributed to C=O of amide I and N—H of amide II (He et al., 2012). The existence of PMMA, PAA, PS, and PDVB in HL particles are confirmed by the C=O stretching band at 1731 cm^{-1}, C=C—H stretching at 3025 cm^{-1}, and C=C stretching at 1600, 1493, and 1453 cm^{-1}, as shown in Spectrum 1C (Nuasaen & Tangboriboonrat, 2013). A broad band at 1731 cm^{-1} indicates an overlap of two carbonyl groups of PMMA (1731 cm^{-1}) and PAA (1705 cm^{-1}) (Canche-Escamilla, Pacheco-Catalan, & Andrade-Canto, 2006; Hu, Wang, & Du, 2012). All mentioned characteristic bands are observed in Spectra 1D and 1E of HL-PEI and HL-chitosan, respectively. Additionally, the N—H bending mode, appeared at 1558 cm^{-1}, confirms the presence of amine groups in both types of amine-functionalized HL particles.

The particle size distribution curves of HL, HL-chitosan, and HL-PEI particles, measured by the DLS technique, are displayed in Fig. 2A. The presence of chitosan and PEI as the outermost layer of particles was confirmed by measuring their zeta potentials at various pHs, and the data are shown in Fig. 2B. The morphologies of

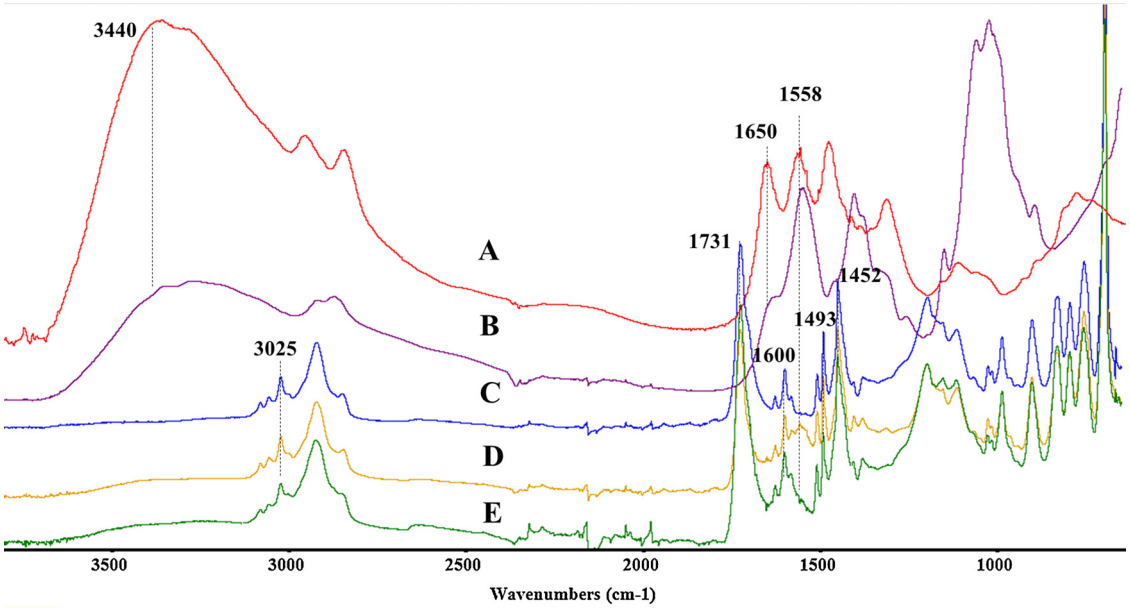

Fig. 1. FTIR spectra of PEI (A), chitosan (B), HL (C), HL-PEI (D) and HL-chitosan (E).

HL, HL-chitosan and HL-PEI particles investigated under TEM are, respectively, presented in Fig. 2C–E.

The larger hydrodynamic volume of HL-chitosan (665 nm) and HL-PEI particles (655 nm), compared to that of HL (530 nm), indicates the presence of chitosan and PEI on HL particles. Although the molecular weight (MW) of chitosan (22,000 g/mol) is much lower than that of PEI (750,000 g/mol), the average sizes of HL-chitosan and HL-PEI are not much different. This might be because the trains of chitosan molecules, having high Tg of 200 °C, are too rigid to lie orderly and closely on the HL surface, while the free loops and tails of chitosan segments are extended away from the surface into aqueous medium (Guo & Gemeinhart, 2008). On the

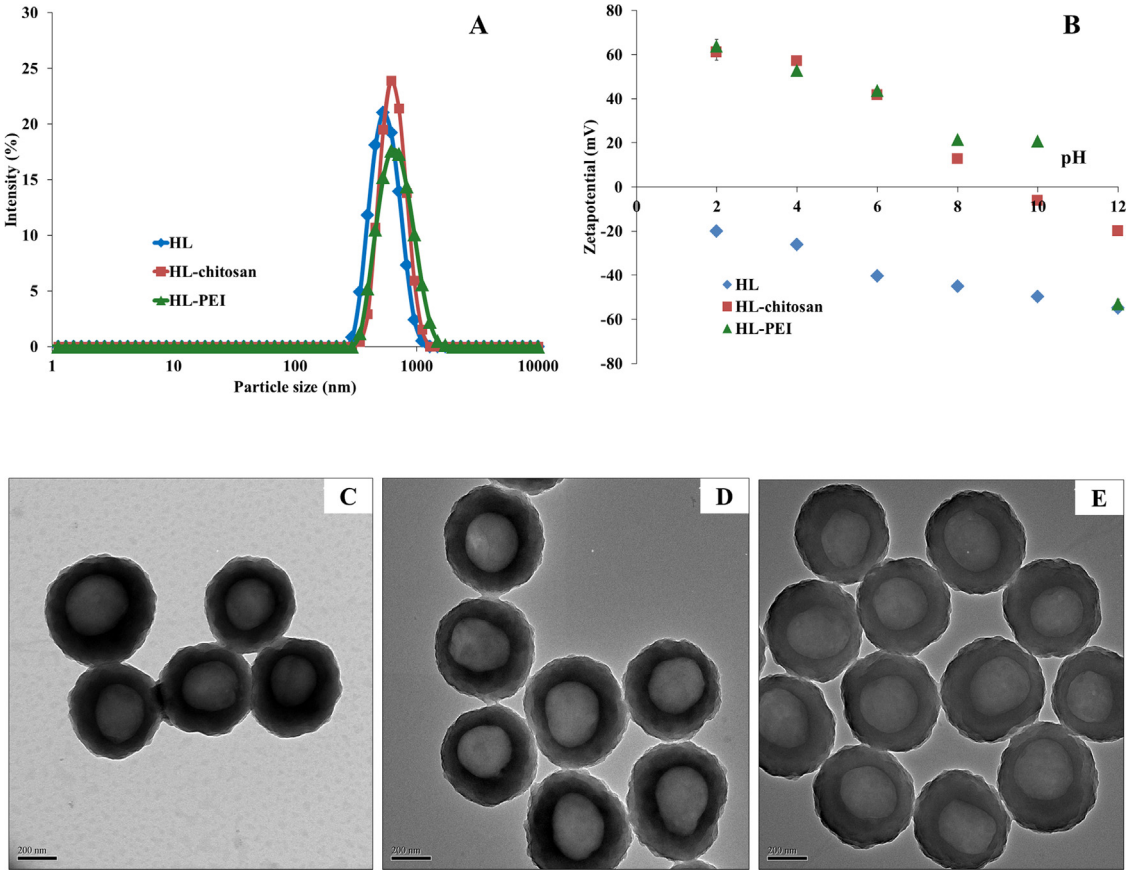

Fig. 2. Particle size (A) and zeta potential (B) of HL, HL-chitosan and HL-PEI particles and TEM images of HL (C) HL-chitosan (D) and HL-PEI (E).

Table 1
Weight compositions, determined from TGA, of HL, HL-chitosan and HL-PEI particles.

Sample	Weight composition (%) at $T_{decomposition}$				Weight (%) of chitosan or PEI in HL
	250	290	445–455	Non-decomposed fraction	
HL	–	–	86.5	8.3	–
HL-chitosan	–	4.5	77.4	12.9	4.8
HL-PEI	12.7	–	72.5	6.1	13.9

contrary, all parts of the highly-flexible branched PEI (liquid at room temperature) can tightly attach onto the HL particle surface. Moreover, chitosan is fully protonated, but PEI is partially protonated while coated on HL particles at pH 5 and 7, respectively (Rinaudo, 2008; Trybala, Szyk-Warszynska, & Warszynski, 2009). Since the secondary (2°) and tertiary (3°) amines of PEI have pKa of 6.7 and 11.6, the higher repulsion between positively-charged chitosan molecules would obstruct the uniform coating of chitosan on HL particles.

In Fig. 2B, the zeta potentials of HL are negative at pH 6–12, as a result of the dissociation of AA monomer to form COO^- groups. The decrease of absolute values from −40.5 mV at pH 6 (COOH, pKa ~4.75) to −26.2 mV at pH 2 is due to the protonation of COO^- of AA (Nuasaen & Tangboriboonrat, 2013). After coating the carboxylated HL with chitosan or PEI, both HL-chitosan and HL-PEI particles possess positive zeta potentials at pH 2–8 and at pH 2–10, because of the protonation of these polymeric amines. Since the branched PEI, composed of 1°, 2° and 3° amines, carries positive charges even in acidic or mild basic environments, the positive charge of HL-PEI at higher pH compared to HL-chitosan is attributed to the protonation of 3° amine (Demadis, Paspalaki, & Theodorou, 2011; Peng, Thio, & Gerhardt, 2010).

TEM micrographs in Fig. 2C–E reveal spherical particles with rough surfaces in all cases. Their average void size is nearly constant at ca. 280 nm, where the particles average diameter increases from 460 nm for HL to ca. 500 nm for the coated HL. The larger particle size confirms the existence of chitosan and PEI on HL-chitosan and HL-PEI surfaces.

The weight compositions of chitosan and PEI coated on HL particles were determined from TGA and DTG thermograms of HL, HL-chitosan and HL-PEI (supplementary data, Fig.S1) and the data are summarized in Table 1.

Supplementary material related to this article can be found, in the online version, at http://dx.doi.org/10.1016/j.carbpol.2013.09.059.

A major weight loss step observed between 360 and 540 °C of all thermograms is due to the decomposition of P(St/AA) and P(MMA/DVB/AA) matrix of HL particles. The important information on the nature of the coating species was obtained at a lower temperature range (200–340 °C), in which those due to PEI and chitosan occurred at 250 and 290 °C, respectively (Jenjob et al., 2012; Wazed Ali, Rajendran, & Joshi, 2011). The weight contents of chitosan and PEI on HL-chitosan and HL-PEI, calculated from TGA thermograms, are ca. 5% and 14%, respectively (Table 1). The

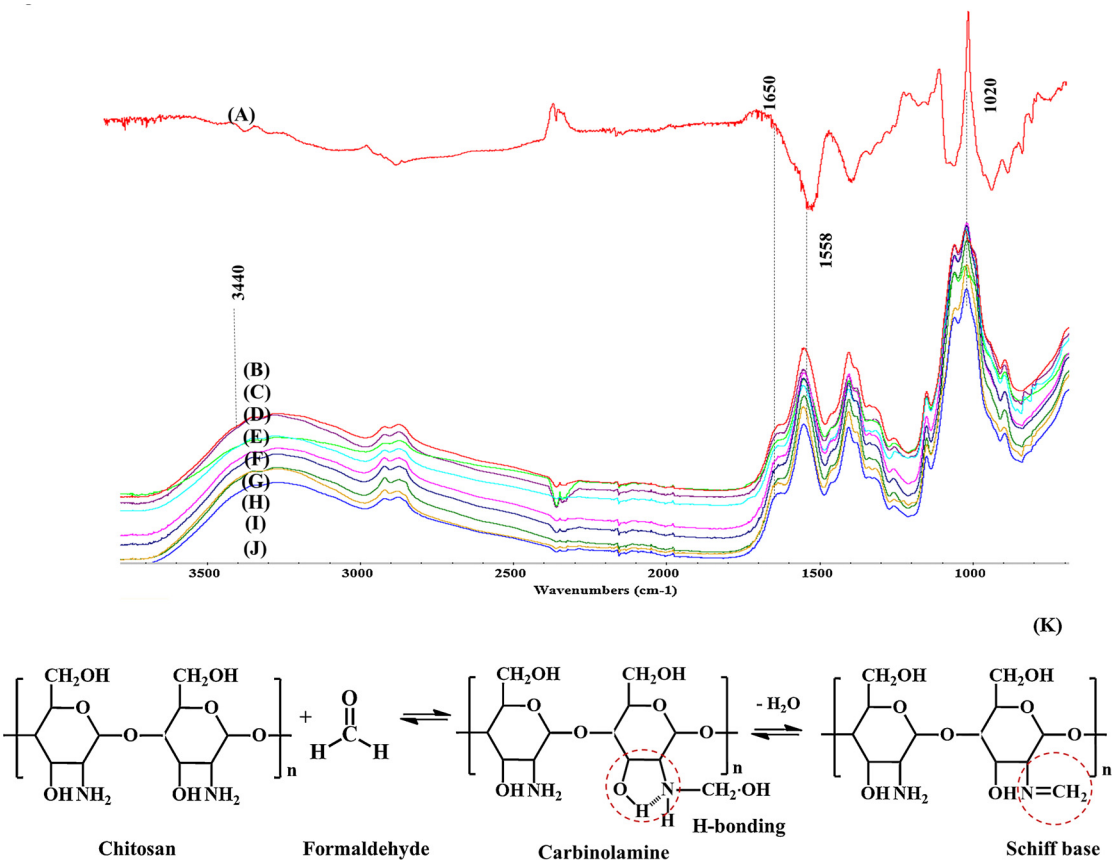

Fig. 3. FTIR spectra of chitosan after formaldehyde adsorption at 0 (B), 5 (C), 15 (D), 30 (E), 45 (F), 60 (G), 75 (H), 90 (I) and 120 min (J), and a different spectrum of chitosan at 120 min adsorption time after subtraction of neat chitosan (A) and reaction between chitosan and formaldehyde (K).

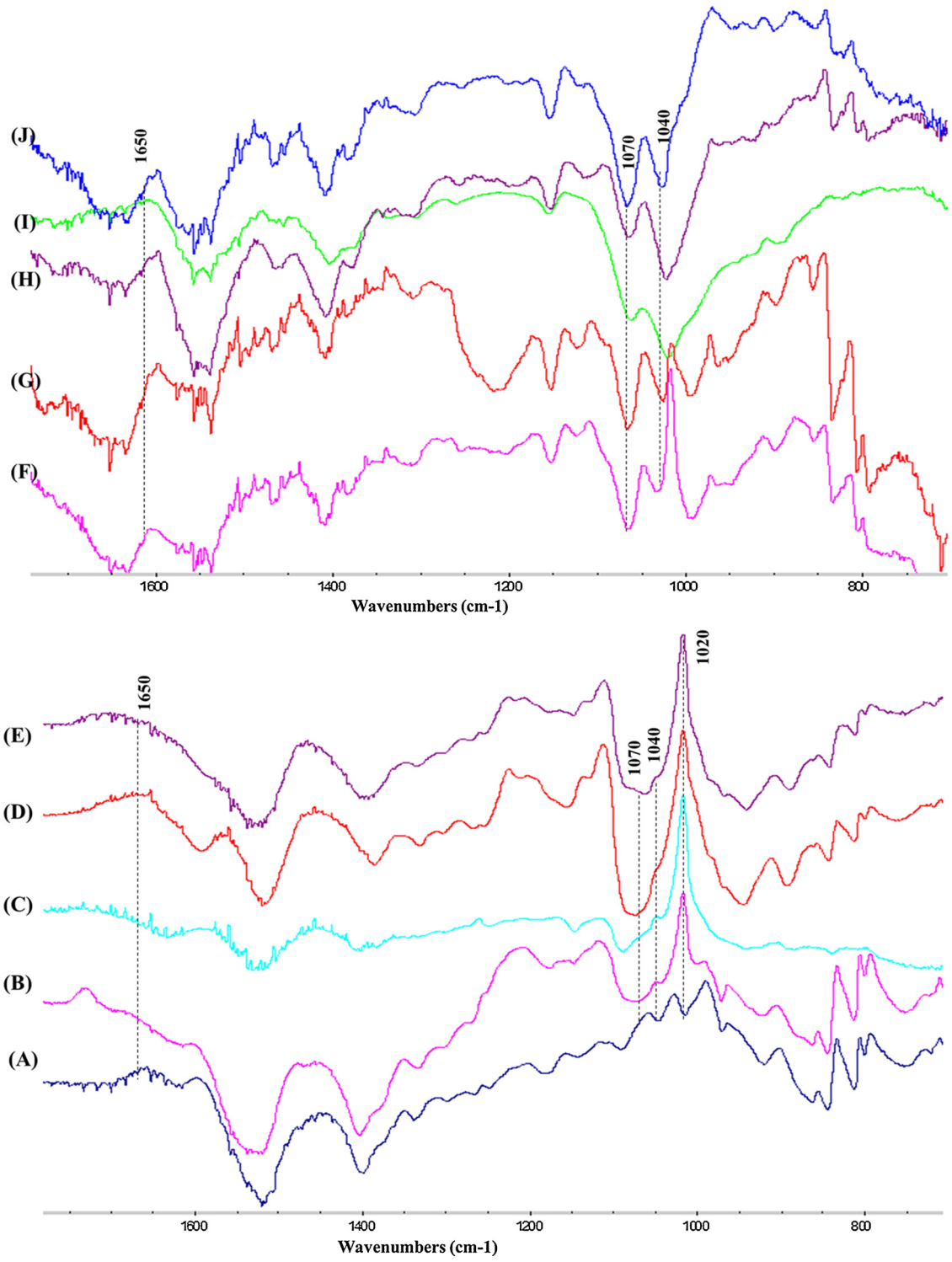

Fig. 4. FTIR different spectra of formaldehyde-adsorbed chitosan at various adsorption times: 5 (A), 30 (B), 60 (C), 90 (D) and 120 min (E) and FTIR different spectra of heat-treated samples after subtraction of formaldehyde-adsorbed chitosan at various adsorption times: 5 (F), 30 (G), 60 (H), 90 (I), 120 min (J).

lower amount of coated chitosan layer on HL particles is likely due to its lower MW, higher rigidity, and full protonation, as earlier stated (Jeng, Dai, Chiu, & Young, 2007; Kaewsaneha, Opaprakasit, Polpanich, Smanmoo, & Tangboriboonrat, 2012; Rinaudo, 2008). In contrast, high MW and flexible branched PEI was partially protonated at pH 7 and, hence, the electrostatically repulsion among their positive charges is lower than that of chitosan, leading to a higher amount of adsorbed PEI (Trybala et al., 2009).

3.2. Formaldehyde adsorption

In formaldehyde adsorption experiments, chitosan, PEI, HL-chitosan, and HL-PEI samples were exposed to saturated formaldehyde vapor for 0, 5, 15, 30, 45, 60, 75, 90, and 120 min. The formaldehyde adsorption characteristics of each sample, as a function of adsorption time, were then examined by FTIR spectroscopy.

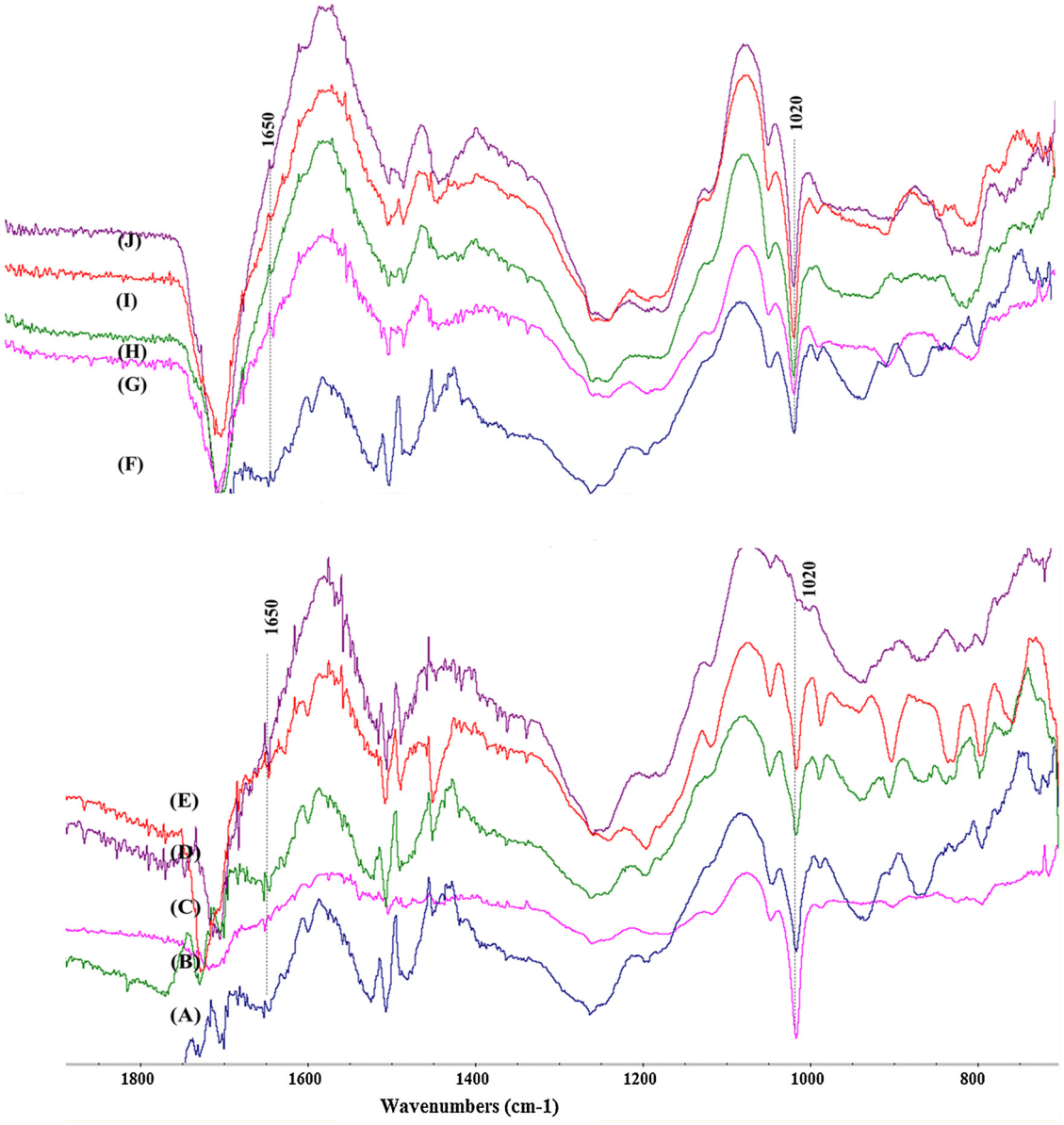

Fig. 5. The different spectra of HL-chitosan at various adsorption times: 0 (A), 5 (B), 45 (C), 90 (D), and 120 (E), after subtraction of HL, and the different spectra of HL-chitosan with a vacuum heat treatment at 0 (F), 5 (G), 45 (H), 90 (I) and 120 min (J), after subtraction of HL.

3.2.1. Formaldehyde adsorption of chitosan and HL-chitosan

Formaldehyde adsorption mechanisms of chitosan are examined by FTIR spectra as a function of adsorption times, as shown in Fig. 3 (Spectra B–J). The reaction of chitosan and formaldehyde is proposed in Fig. 3K.

Changes on all characteristic bands at 3440 (O—H and N—H stretching), 1650 (C=O of amide I) and 1558 cm^{-1} (N—H of amide II) of chitosan, after formaldehyde adsorption (Spectra 3C–J), are similar to those of neat chitosan (Spectrum 3B) (He et al., 2012). However, the intensity of the 1020 cm^{-1} band increases with increasing formaldehyde adsorption time, due to the chemical reaction of chitosan and formaldehyde. To recognize the change of chitosan, a different FTIR spectrum after a subtraction of neat chitosan from the formaldehyde-adsorbed chitosan at 120 min was generated, as displayed in Spectrum 3A. The appearance of a negative band at 1558 cm^{-1} (—NH bending of amide II) and a positive band at 1650 cm^{-1} (—C=N of azomethine or Schiff base) indicate a nucleophilic addition of amines of chitosan to carbonyl of formaldehyde, followed by an elimination of water (H_2O), as proposed in Fig. 3K (Knaul, Hudson, & Creber, 1999; Zhu, Li, Zheng, Xu, & Li, 2012). It is noted that the characteristic band of amide bonds in chitin (amide I) and that of the Schiff base are both located near 1650 cm^{-1} (Spectra 3A–J) (He et al., 2012). This absorption band can also indicate carbonyl group of N-acyl chitosan, occurred from the reaction between chitosan and acid anhydride (Muzzarelli, 1977).

In addition, a sharp positive different band at 1020 cm^{-1} (aliphatic C—N), corresponding to carbinolamine intermediate, was also observed (Spectrum 3A) (Farris, Song, & Huang, 2010; Nishat, Khan, Rasool, & Parveen, 2011). This was possibly because the reaction between chitosan and formaldehyde generated not only the Schiff base, but also other intermediate products, which are then transformed to Schiff base structure by dehydration (Fig. 3K). However, the high stability of these five-membered ring intermediates, due to intra-molecular H-bonding of carbinolamine, might retard their transformation. In general, the high efficiency of Schiff base formation was achieved by using highly electrophilic carbonyl compounds and strong nucleophilic amines in the absence of electronic and steric factors (Chakraborti, Bhagat, & Rudrawar, 2004).

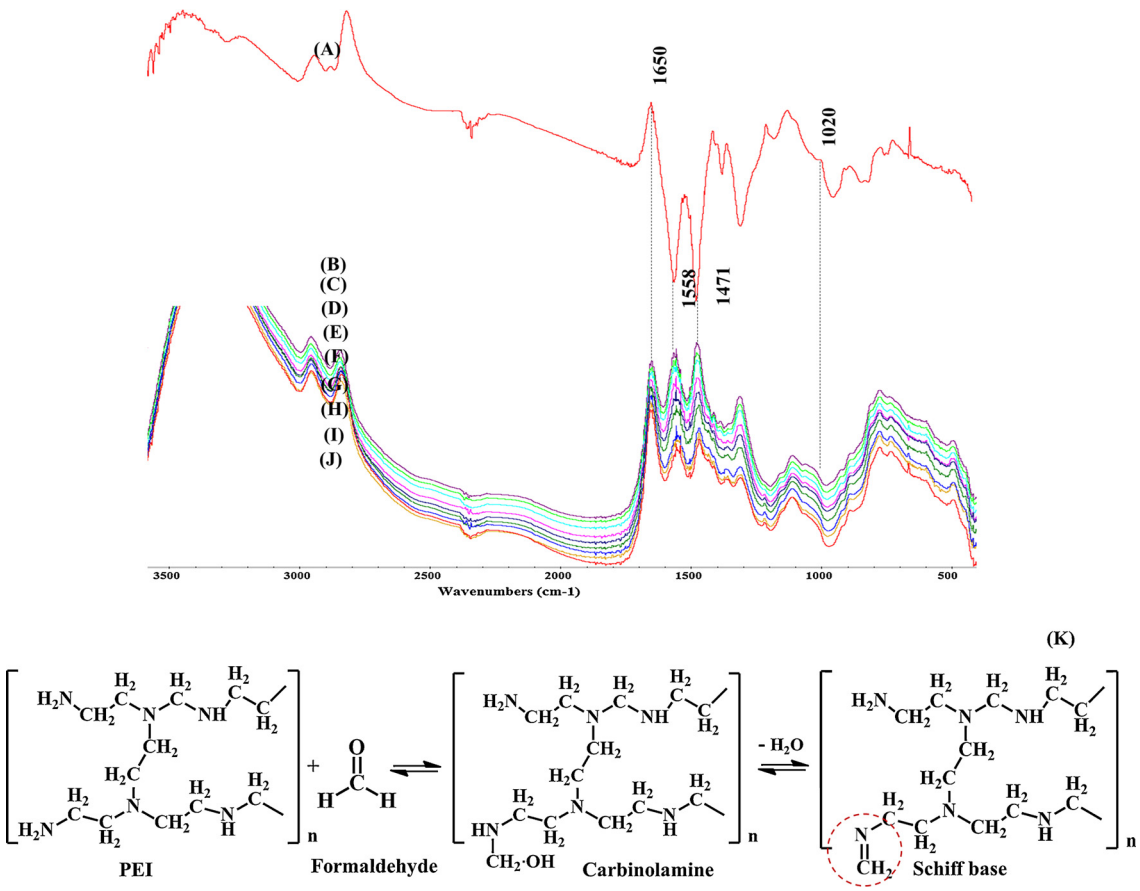

Fig. 6. FTIR spectra of PEI at various formaldehyde adsorption times: 0 (B), 5 (C), 15 (D), 30 (E), 45 (F), 60 (G), 75 (H), 90 (I) and 120 min (J), and the different spectrum of PEI at 120 min after subtraction of neat PEI (A) and reaction between PEI and formaldehyde (K).

Since the free lone pair electrons of N atom of carbinolamine are engaged in the H-bonded structure, the nucleophilicity of amine groups decreases. In the absence of acid protonation, the reaction involved a bad hydroxyl (—OH) leaving group. Therefore, the more stable intermediates, indicated by the 1020 cm^{-1} band, occurs at high yields compared to the Schiff base structure at 1650 cm^{-1}, as the dehydration of carbinolamine at neutral pH was the rate determination step (Brown, 1999). This was reflected in the different FTIR spectra of the adsorbed samples at various times after subtraction of neat chitosan, as shown in Fig. 4 (Spectra A–E).

It was also found that the amounts of intermediate (1020 cm^{-1} band) increase with an increase of adsorption time from 5 to 90 min, and remained constant, reflecting a complete consumption of the chitosan amines (Spectra 4A–E). As mentioned above, the reaction proceeded in excellent yields within a short time period (Chakraborti et al., 2004). The negative different patterns at 1070 and 1040 cm^{-1} indicate the conversion of chitosan amines.

In order to prove the transformation of intermediates to Schiff base, the formaldehyde adsorbed chitosan samples at various adsorption times were heated in a vacuum oven at 50 °C for 120 min to facilitate the dehydration, and their FTIR spectra were re-examined. The different spectra generated from the subtraction of formaldehyde adsorbed chitosan at various times from those of the vacuum-heat treatment are shown in Fig. 4 (Spectra F–J). The absence of the positive different band at 1020 cm^{-1} reflects the transformation of carbinolamine intermediate to Schiff base structure by a removal of H_2O. The appearances of positive band at 1650 cm^{-1} and the negative patterns at 1070 and 1040 cm^{-1} indicate the conversion of amines to Schiff base structure.

FTIR spectra of HL and HL-chitosan at various formaldehyde adsorption times were examined (presented as supplementary data, Fig.S2). The variation of characteristic bands of HL-chitosan, i.e., C=O stretching at 1731 cm^{-1}, C=C stretching at 1600, 1493, and 1453 cm^{-1} and a shoulder peak of N—H bending at 1558 cm^{-1} at all formaldehyde adsorption times cannot be clearly observed. However, the intensity of the 1020 cm^{-1} band decreases after coating with chitosan. When HL-chitosan was subjected to formaldehyde adsorption, the band intensity at 1020 cm^{-1} slowly increases with increasing the adsorption time from 0 to 120 min.

Supplementary material related to this article can be found, in the online version, at http://dx.doi.org/10.1016/j.carbpol.2013.09.059.

To explain these results, the spectra of HL-chitosan at various adsorption times were subtracted by that of the original HL, as shown in Fig. 5 (Spectra A–E).

The different FTIR spectra at 0 and 5 min (Spectra 5A and B) display an intense negative pattern at 1020 cm^{-1}. The negative intensity largely decreases when the adsorption time was prolonged from 5 to 120 min (Spectra 5B–E). Meanwhile, a positive different mode presenting as a broad band centered near 1600 cm^{-1} represents the Schiff base formation (Spectra 5B–E). The results agree well with the uptake of formaldehyde by chitosan particles, i.e., the absorption peak of Schiff base slightly shifts to lower wavenumber (Zhou et al., 2013). The positive pattern increases in intensity with increasing adsorption time, likely a result from the increase in carbinolamine and Schiff base contents, as a function of reaction time with formaldehyde.

Similar to the experiments on chitosan, HL-chitosan samples after formaldehyde adsorption were also heat treated at 50 °C

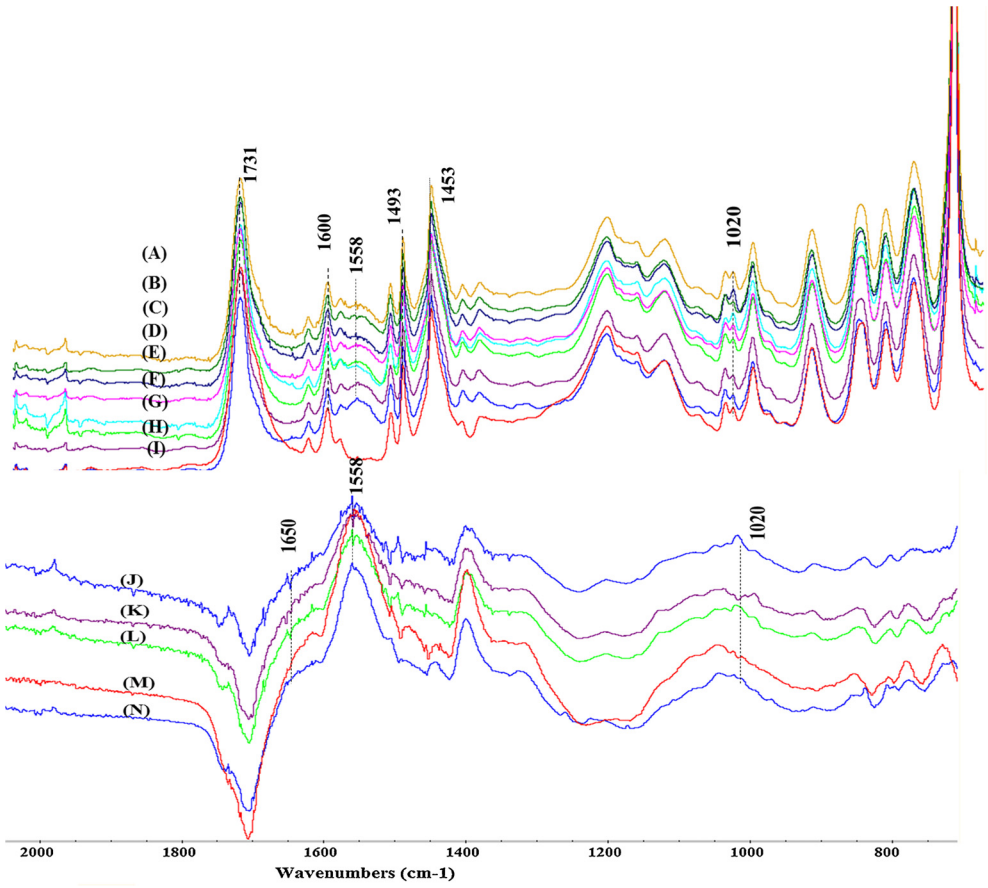

Fig. 7. FTIR spectra of HL-PEI at various adsorption times: 120 (A), 90 (B), 75 (C), 60 (D), 45 (E), 30 (F), 15 (G) and 0 min (H) and HL (I), their different spectra at 120 (J), 90 (K), 60 (L), 5 (M) and 0 min (N), after subtraction of HL.

under vacuum. FTIR spectra of HL-chitosan particles at various formaldehyde adsorption times are presented as supplementary data, Fig.S3. The different spectra obtained from subtraction of the heat-treated HL-chitosan by HL, as shown in Fig. 5 (Spectra 5F–J), obviously indicate that the intensity of Schiff base band at 1650 cm^{-1} increases, compared to that obtained at the same adsorption time, before the heat treatment (Spectra 5A–E). The negative different band at 1020 cm^{-1}, however, shows a nearly constant intensity, regardless of adsorption time (Spectra 5F–J). This suggests that most of carbinolamine intermediate species, generated from the reaction of formaldehyde and chitosan on HL-chitosan particles, at any adsorption time, are converted to Schiff base by dehydration. The results are in good agreement with the chitosan model.

Supplementary material related to this article can be found, in the online version, at http://dx.doi.org/10.1016/j.carbpol.2013.09.059.

3.2.2. Formaldehyde adsorption of PEI and HL-PEI

FTIR spectra of PEI at various formaldehyde adsorption times and a different spectrum of PEI at 120 min after subtraction of neat PEI are presented in Fig. 6 (Spectra A–J). The reaction of PEI and formaldehyde are proposed in Fig. 6K.

Spectra 6B–J show that the intensities of the 1558 and 1471 cm^{-1} modes, corresponding to —NH bending of 1° amine and —N^+H of 1° or 2° amines, decrease with increasing formaldehyde adsorption time. This indicates a reaction of 1° and 2° amines with formaldehyde (Gesser & Fu, 1990).

Unlike chitosan, the different FTIR spectrum derived from PEI at 120 min adsorption time reveals a positive Schiff base band at 1650 cm^{-1}, whereas a negative pattern of the intermediate structure at 1020 cm^{-1} is not clearly observed, as shown in Spectrum 6A. The corresponding different spectra of PEI at all adsorption times show similar characteristics (supplementary data, Fig.S4). The intensity of the positive different band of the Schiff base at 1650 cm^{-1} increases with increasing adsorption time, whereas the band intensities of the 1558 and 1471 cm^{-1} modes, corresponding to —NH bending of 1° amine and —N^+H of 1° or 2° amines, decreases. This suggests that the formation of Schiff bases via nucleophilic addition of 1° and 2° amines of branched PEI to the carbonyl group of formaldehyde followed by dehydration is preferable, compared to chitosan, due to its low degree of intra-molecular H-bonding as illustrated in Fig. 6K (Chakraborti et al., 2004).

Supplementary material related to this article can be found, in the online version, at http://dx.doi.org/10.1016/j.carbpol.2013.09.059.

For HL-PEI, the variation in the characteristic band of C=O stretching at 1731 cm^{-1}, C=C stretching at 1600, 1493, and 1453 cm^{-1}, and N—H bending at 1558 cm^{-1} after formaldehyde adsorption at various times from 0 to 120 min is not clearly detected in Fig. 7 (Spectra A–I). The corresponding FTIR different spectra are shown in Spectra J-N, where a positive pattern attributed to the formation of Schiff base at 1650 cm^{-1}, is observed as a shoulder band.

The low positive intensity of the intermediate characteristic at 1020 cm^{-1} is also noticed. In contrast to that of neat PEI model, the characteristic bands of the Schiff base product are not clearly observed in HL-PEI. This is possibly due to a small amount of 1° amine presented in branched PEI (35, 37 and 28 wt% for 1°, 2° and 3° amines, respectively), and low reactivity of its 2° amines

caused from steric effect (Gesser & Fu, 1990). However, a decrease in intensity of a positive different band of N—H bending mode (1558 cm^{-1}) with time from 0 to 120 min in Spectra 7J-N confirms the progress of reaction between PEI on HL-PEI surface with formaldehyde.

4. Conclusions

HL-chitosan and HL-PEI particles, prepared by the seeded emulsion polymerization and the LbL technique, can chemically adsorb formaldehyde via the nucleophilic addition of amines to carbonyls of formaldehyde, followed by the elimination of water molecules. FTIR spectra reveal that the two species, i.e., carbinolamine intermediate and Schiff base, are generated when HL-chitosan is used in formaldehyde adsorption tests, whereas, the Schiff base structure is not clearly observed in HL-PEI. In both cases, the adsorbent activity increases with increasing formaldehyde adsorption time. The transformation of intermediate to Schiff base can be accelerated by increase of temperature. Further modifications of multilayer HL-chitosan particles could lead to a special indoor coating material.

Acknowledgements

Research Grant (RTA5480007) from The Thailand Research Fund (TRF)/Commission on Higher Education to P.T. and a scholarship from TRF through the Royal Golden Jubilee Ph.D. Program (Grant No. PHD/0190/2553) to S.N. are gratefully acknowledged.

References

Agudo, S., Polo, A. C., Bernal, M. P., Coronas, J., & Santamaria, J. (2004). Removal of pollutants from indoor air using zeolite membranes. *Journal of Membrane Science*, *240*, 159–166.

Bourgeat-Lami, E. (2003). Hollow particle synthetic pathways and potential applications. In A. Elaissari (Ed.), *Colloidal polymers: Synthesis and characterization* (pp. 189–223). Marcel Dekker.

Brown, K. H. (1999). *Kinetic studies on the reaction of formaldehyde with amines in the presence of sulfite (Durham theses)*. Durham University.

Canche-Escamilla, G., Pacheco-Catalan, D. E., & Andrade-Canto, S. B. (2006). Modification of properties of rayon fibre by graft copolymerization with acrylic monomer. *Journal of Materials Science*, *41*, 7296–7301.

Chakraborti, A. K., Bhagat, S., & Rudrawar, S. (2004). Magnesium perchlorate as an efficient catalyst for the synthesis of imines and phenylhydrazones. *Tetrahedron Letters*, *45*, 7641–7644.

Cogliano, V. J., Grosse, Y., Baan, R. A., Straif, K., Secretan, M. B., El Ghissassi, F., et al. (2005). Meeting report: Summary of IARC monographs on formaldehyde, 2-butoxyethanol, and 1-tert-butoxy-2-propanol. *Environmental Health Perspectives*, *113*, 1205–1208.

Da Silva, C. M., Da Silva, D. L., Modolo, L. V., Alves, R. B., de Resende, M. A., Martins, C. V. B., et al. (2011). Schiff bases: A short review of their antimicrobial activities. *Journal of Advanced Research*, *2*, 1–8.

Demadis, K. D., Paspalaki, M., & Theodorou, J. (2011). Controlled release of bis(phosphonate) pharmaceuticals from cationic biodegradable polymeric matrices. *Industrial & Engineering Chemistry Research*, *50*, 5873–5876.

Du, P., Liu, P., Mu, B., & Wang, Y. (2010). Monodisperse superparamagnetic pH-sensitive single-layer chitosan hollow microsphere with controllable structure. *Journal of Polymer Science Part A: Polymer Chemistry*, *48*, 4981–4988.

Farris, S., Song, J., & Huang, Q. (2010). Alternative reaction mechanism for the cross-linking of gelatin with glutaraldehyde. *Journal of Agricultural and Food Chemistry*, *58*, 998-103

Formaldehyde TEACH Chemical Summary, US Environmental Protection Agency. http://www.epa.gov/teach/chem_summ/Formaldehyde_summary.pdf Accessed on June, 2013.

Gesser, H. D., & Fu, S. (1990). Removal of aldehydes and acidic pollutants from indoor air. *Environmental Science & Technology*, *24*, 495–497.

Guo, C., & Gemeinhart, R. A. (2008). Understanding the adsorption mechanism of chitosan onto poly(lactide-co-glycolide) particles. *European Journal of Pharmaceutics and Biopharmaceutics*, *70*, 597–604.

Heack, Hd'A., Casanova-Schmitz, M., Dodd, P. B., Schachter, E. N., Witek, T. J., & Tosun, T. (1985). Formaldehyde (CH_2O) concentration in the blood of humans and Fischer-344 rats exposed to CH_2O under controlled conditions. *American Industrial Hygiene Association Journal*, *46*, 1–3.

He, G., Wang, Z., Zheng, H., Yin, Y., Xiong, X., & Lin, R. (2012). Preparation, characterization and properties of aminoethyl chitin hydrogels. *Carbohydrate Polymers*, *90*, 1614–1619.

Hu, H., Wang, H., & Du, Q. (2012). Preparation of pH-sensitive polyacrylic acid hollow microspheres and their release properties. *Soft Matter*, *8*, 2816–2822.

Jeng, J., Dai, C. A., Chiu, W. Y., & Young, P. Y. (2007). Effect of cationic surfactant on homogenization and polymerization of methyl methacrylate miniemulsion modified by chitosan. *Polymer International*, *56*, 746–753.

Jenjob, S., Tharawut, T., & Sunintaboon, P. (2012). Facile synthesis of silver immobilized-poly(methyl methacrylate)/polyethyleneimine core–shell particle composite. *Materials Science and Engineering C*, *32*, 2068–2072.

Kaewsaneha, C., Opaprakasit, P., Polpanich, D., Smanmoo, S., & Tangboriboonrat, P. (2012). Immobilization of fluorescein isothiocyanate on magnetic polymeric nanoparticle using chitosan as spacer. *Journal of Colloid and Interface Science*, *377*, 145–152.

Knaul, O. Z., Hudson, S. M., & Creber, K. A. M. (1999). Crosslinking of chitosan fibers with dialdehydes: Proposal of a new reaction mechanism. *Journal of Polymer Science Part B: Polymer Physics*, *37*, 1079–1094.

McDonald, C. J., & Devon, M. J. (2002). Hollow latex particles: Synthesis and applications. *Advances in Colloid and Interface Science*, *99*, 181–213.

Muzzarelli, R. A. A. (1977). *Chitin*. Oxford: Pergamon Press., pp.132

Nishat, N., Khan, S. A., Rasool, R., & Parveen, S. (2011). Synthesis, spectral characterization and biocidal activity of thermally stable polymeric Schiff base and its polymer metal complexes. *Journal of Inorganic and Organometallic Polymers*, *21*, 673–681.

Nuasaen, S., & Tangboriboonrat, P. (2013). Highly charged hollow latex particles prepared via seeded emulsion polymerization. *Journal of Colloid and Interface Science*, *396*, 75–82.

Nypelo, T., Osterberg, M., Zu, X., & Laine, J. (2011). Preparation of ultra thin coating layers using surface modified silica nanoparticles. *Colloids and Surfaces A: Physicochemical and Engineering Aspects*, *392*, 313–321.

Obee, T. N., & Brown, R. T. (1995). TiO_2 photocatalysis for indoor air applications: Effects of humidity and trace contaminant levels on the oxidation rates of formaldehyde, toluene, and 1,3-butadiene. *Environmental Science & Technology*, *29*, 1223–1231.

Peng, C., Thio, Y. S., & Gerhardt, R. A. (2010). Enhancing the layer-by-layer assembly of indium tin oxide thin films by using polyethyleneimine. *Journal of Physical Chemistry C*, *114*, 9685–9692.

Polpanich, D., Tangboriboonrat, P., & Elaissari, A. (2005). The effect of acrylic acid amount on the colloidal properties of polystyrene latex. *Colloid & Polymer Science*, *284*, 183–191.

Rinaudo, M. (2008). Main properties and current applications of some polysaccharides as biomaterials. *Polymer International*, *57*, 397–430.

Silva, C. A., & Galembeck, F. (2010). Void formation and opacity in latex films with aluminum phosphate particles. *Colloids and Surfaces A: Physicochemical and Engineering Aspects*, *363*, 146–154.

Trybala, A., Szyk-Warszynska, L., & Warszynski, P. (2009). The effect of anchoring PEI layer on the build-up of polyelectrolyte multilayer films at homogeneous and heterogeneous surfaces. *Colloids and Surfaces A: Physicochemical and Engineering Aspects*, *343*, 127–132.

Wada, T., Uragami, T., & Matoba, Y. (2005). Chitosan-hybridized acrylic resins prepared in emulsion polymerizations and their application as interior finishing coating. *Journal of Coating Technology and Research*, *2*, 577–582.

Wang, X., Cui, F., Lin, J., Ding, B., Yu, J., & Al-Deyab, S. S. (2012). Functionalized nanoporous TiO_2 fibers on quartz crystal microbalance platform for formaldehyde sensor. *Sensors and Actuators B: Chemical*, *171-172*, 658–665.

Wazed Ali, S., Rajendran, S., & Joshi, M. (2011). Synthesis and characterization of chitosan and silver loaded chitosan nanoparticles for bioactive polyester. *Carbohydrate Polymers*, *83*, 438–446.

Yang, K., Liu, Y., Yu, C., & Chen, B. (2011). Fabrication of chitosan/silver nanocomposites based on electrochemical methods for removing formaldehyde in air. *Materials Chemistry and Physics*, *126*, 993–997.

Zhou, X., Cheng, X. J., Liu, W. F., Li, J., Ren, L. H., Dang, Q. F., et al. (2013). Optimization and characteristics of preparing chitosan microspheres using response surface methodology. *Journal of Applied Polymer Science*, *127*, 4433–4439.

Zhu, Y., Li, H., Zheng, Q., Xu, J., & Li, X. (2012). Amine-functionalized SBA-15 with uniform morphology and well-defined mesostructure for highly sensitive chemosensors to detect formaldehyde vapor. *Langmuir*, *28*, 7843–7850.